IJBPAS, August, 2015, 4(8): 5663-5679

ISSN: 2277–4998

International Journal of Biology, Pharmacy and Allied Sciences (IJBPAS)

'A Bridge Between Laboratory and Reader'

www.ijbpas.com

SYNTHESIS, GROWTH MECHANISMAND ANTIFUNGAL ACTIVITY OF ZNO NANOSTRUCTURES GROWN VIA A NOVEL ATMOSPHERIC PRESSURE SOLUTION EVAPORATION METHOD

M. HAMDAM MOMEN, A. AMADEH*, M. HEYDARZADEH SOHI

School of Metallurgy and Materials Engineering, College of Engineering, University of Tehran, P.O. Box 11155-4563, Tehran, Iran.

***Corresponding Author: Email: Amadeh@ut.ac.ir; Tel: +98(21)82084609, Fax: +98(21)88006076**

ABSTRACT

In this study, a novel method called "atmospheric pressure solution evaporation (APSE)" was developed for growing of ZnO nanostructures on Al_2O_3 surface. The growth of ZnO nanostructureson $Al_2O_3$was performed at three temperatures of 300, 400 and 500 °C. Field emission scanning electron microscopy (FESEM) demonstrated that ZnO nanostructures formed in nanorods or cauliflower- like rod based on the growth temperature. X-ray diffraction patterns of ZnO nanostructures prepared at different growth temperatures were indexed as hexagonalWurtzite structure without any impurity. The optical band gap energy evaluated by diffuse reflectance spectroscopy (DRS) was 3.22~3.29 eV. The degradation of Methylene Blue (MB) dye demonstrated that Zn Onanorods grown at the growth temperature of 300 °C showed better photodegradation in comparison with other nanostructures. Antifungal properties of ZnOnanorods against *Candida albicans*, were much higher than that of other nanostructures. Finally, the growth mechanism based on hydrolysis and condensation was proposed.

Keywords: Znonanostructures; atmospheric pressure solvent evaporation (APSE); growth temperature; photodegradation; Antifungal

INTRODUCTION

Zinc oxide (ZnO) is extensively used in photo-degradation of toxic organic pollutants and solving environmental problems due to its wide direct band gap (about 3.3 eV) and large excitation binding energy (about 60 meV). Furthermore, ZnO as a non-toxic and inexpensive material has presented good mechanical, chemical and thermal stability[1, 2].The use of ZnO as antibacterial and antifungal agent has the advantages of improved safety and stability as compared with organic antimicrobial agents[3],which makes it appropriate for use in food industries, water and wastewater treatment etc.

Various morphologies of ZnO nanostructures such as nanoparticles, nanorods, nanowires, nanotubes, nanobelts,nanoribbons and nanosheets, were synthesized by various physical and chemical preparation methods[4-7].These nanosizedZnO presents higher photocatalytic and antimicrobial activity compared to bulk ZnO but their synthesis methods regularly require high temperatures, high purity precursors, high vacuum or difficult process.

In this research, a simple novel method called "atmospheric pressure solution evaporation (APSE)" was developed for synthesis of highly crystalline ZnO nanostructures and the effect of growth temperature on photocatalytic and antifungal properties was studied. This method, compared to other synthesis methods, offers several advantages such as simplicity, cost-effective,low-temperature, atmospheric pressure and large area deposition.

MATERIALS AND METHODS

Zinc oxide nanostructures were grown on the basis of atmospheric pressure solution evaporation method. The growth of ZnO nanostructures from evaporated solution was performed on Al_2O_3 surface at three temperatures of 300, 400 and 500 °C. Al_2O_3 thin films were prepared on glass substrates via dip coating process. For this purpose, alumina powder (KMS-92, Martinswerk) was suspended in water and it was stirred for 24 hours. The glass substrates were then dip coated by thin alumina layers.The alumina coated glasses were then dried in an oven at 60 °C for 12 hours.

Zinc oxide nanostructures were grown on Al_2O_3 layer by solution evaporation method. The solution was prepared by dissolving zinc acetate dehydrate (Merck) in deionized water (0.22 M). Polyvinylpyrrolidone (PVP) (Merck) was added as a surfactant with weight ratio of 1:10 of PVP:Zn. The solution was placed on a heater and it was stirred until

the solution temperature reached at 70 ℃. The solution temperature was hold at 70 ℃ until the solution volume reduced to one-third of its initial volume and a small amount of zinc acetate and PVP gel was obtained. This solution was poured into a ceramic crucible and the coated substrates were placed on top of it. The ceramic crucible was then placed into an electric furnace. The samples were heated at a rate of 3 °C/min to 300, 400 and 500 ℃, respectively and cooled down to room temperature. Schematic of the growth process of ZnOnanorods on Al_2O_3 substrate is shown in Fig.1.

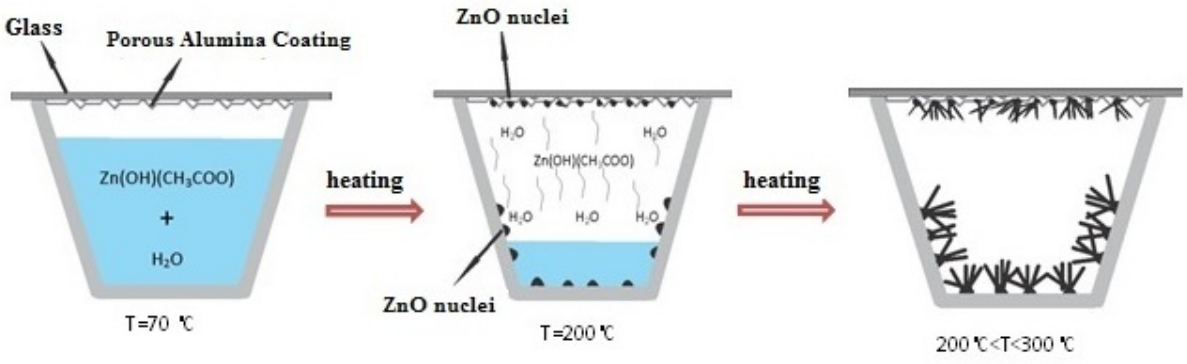

Fig. 1: The Scheme of the growth process.

Field emission scanning electron microscopy (FE-SEM, S4160 Hitachi Japan) was used to study the microstructure and morphology of the samples. The phase structure and crystallite size of grown nanostructures were investigated by X-ray diffraction technique (XRD, Philips Expert- MPD) using Cu-Kα radiation with wavelength of 1.5439Å. The crystallite size of ZnO nanostructures was measured according to Scherrer equation ($D=0.94\lambda/\beta \cos\theta$) where λ is the wavelength of X-ray, β is full width at half maximum intensity (FWHM) in radians and θ is the Bragg angle.

The specific surface area was measured by nitrogen adsorption at -195.8 °C using the BET equation (PhysisorptionAnalyzer, ASAP 2020, Micromeritics).

The optical characteristics of samples were analyzed by UV-Vis spectroscopy using the wavelength range of 190-1000 nm and diffuse reflectance spectra (DRS). To investigate the photocatalytic activity of the samples, the prepared ZnO nanostructures grown on Al_2O_3 coated substrate were placed in a petri dish containing 10 ml of 5 ppm aqueous solution of MB. The petri dish was placed in a homemade box. The sample was then irradiated by a UV source (Osram, 400 W

high-pressure Hg lamp) with prominent emission at 365 nm. The distance of lamp from reaction system was 1 cm and the temperature was fixed at 25 °C. After UV-radiation, the concentration of MB solution was measured by UV-Visible spectrophotometer (Hitachi U-2000). The change in the concentration of MB was measured at regular intervals of time.

RESULTS AND DISCUSSION

3.1. Morphological properties

The FE-SEM images of the grown structures, shown in Fig. 2, indicate that high-density ZnO nanostructures are successfully obtained on Al_2O_3substrates, i.e. α- Al_2O_3 provides appropriate sites for nucleation and growth of ZnO. As shown in Fig.2a dense vertically aligned hexagonal urchin-shaped faceted nanorods with a diameter range of 30–70nm grow at temperature of 300°C overa large area of thesubstrate. As the growth temperatureincreases (Fig.2 b and c), ZnOmorphology changes from nanorod to a cauliflower- like structure.The size of cauliflower rods is in the range of 150–250 nm and 200–300 nm at 400 and 500 °C, respectively. The density of cauliflower rods is decreased comparing to Fig. 2a. This evolution can be attributed to the difference in nucleation and growth mechanism of ZnO particles at different growth temperatures[8]discussed in Section 3.5.

3.2 Structural properties

Fig. 3 shows X-ray diffraction patterns of ZnO nanostructures prepared at different growth temperatures. All diffraction peaks can be indexed as hexagonal Wurtzite structure without any impurity (ICSD75-0576, a= 3.242 A˚, c= 5.194 A˚). The strong intensity of (002) peak in Fig. 3 indicates the high crystalline quality as well as the highly oriented nature of ZnOnanorods.

It is reported that the intensity ratio of (002) polar planes to (100) nonpolar planes (I (002)/I (100)) can influence the photocatalytic activitybecause the polar planes of ZnO help the formation of oxygen vacancies[9]. This factor is presented in Tab. 1.According to XRD results, when the growth temperature is 300 °C, the intensity of (002) peak is higher than (100) peaks, which means that c-axis growth is dominant[10]. However, when the growth temperature increases, the preferred growth direction changes progressively to (100) direction, showing that the growth mode changes fromone-dimensional (1D) growth to two-dimensional (2D) growth.Moreover, according to Fig. 3, the full width at half maximum (FWHM) of diffraction peaks decreases as the growth

temperature increases. So, based on the Scherrer equation[7], a finer crystallite size can be expected at 300 °Cwith respect to 400 and 500 °C (presented in Tab. 1.) which confirms the result of FE-SEM micrographs.

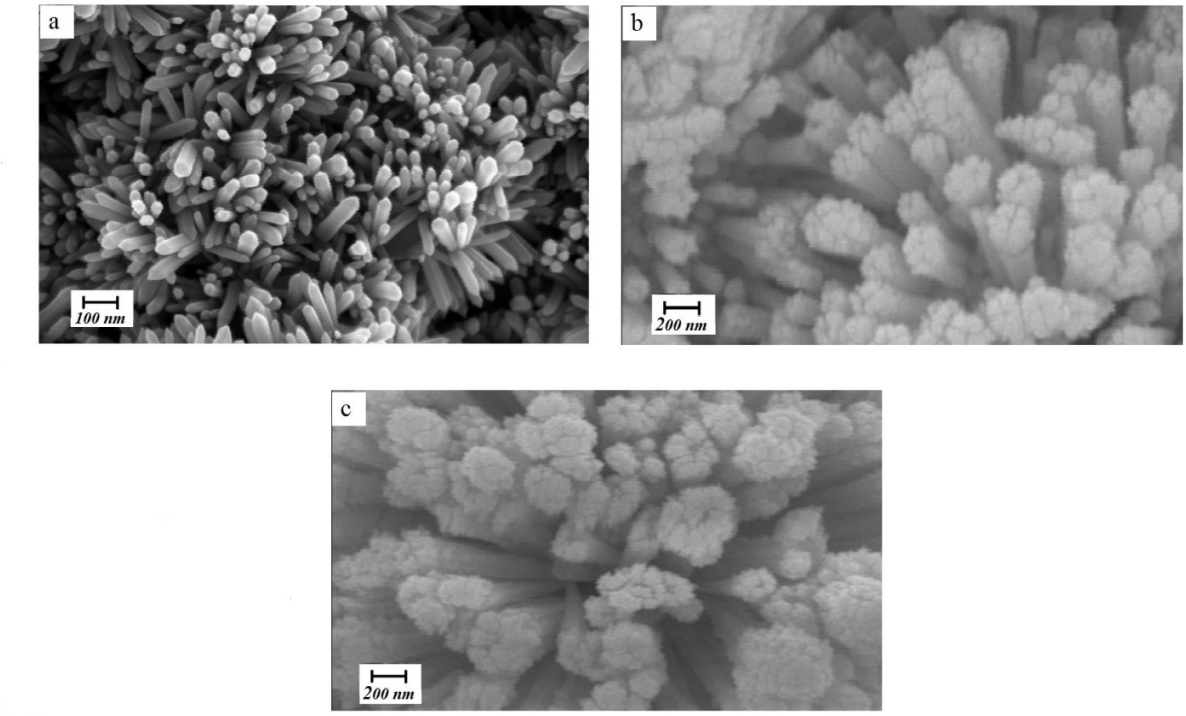

Fig. 2. FE-SEM images of ZnO structures grown on α-Al2O3coated substrates at different growth temperatures: a) 300; b) 400 and c) 500 °C.

The results of specific surface area (SSA) measured by BET are also shown in Tab. 1. The results show that as the growth temperature is increased, the SSA decreases. A high SSA leads toincrease active site numbers on the surface of photocatalystand consequently more rapid reaction rate of photo-generated charge carriers and so that it improves the photocatalytic degradation efficiency of organic pollutants [11].

Table 1. The mean crystallite size, ratio of (002) plane to (100) plane and surface area of ZnO samples

Growth temperature (°C)	Mean crystallite size (nm)	I (002)/I (100)	BET surface area (m^2/g)
300	45	1.28	10.07
400	59	1.10	6.71
500	67	0.91	5.43

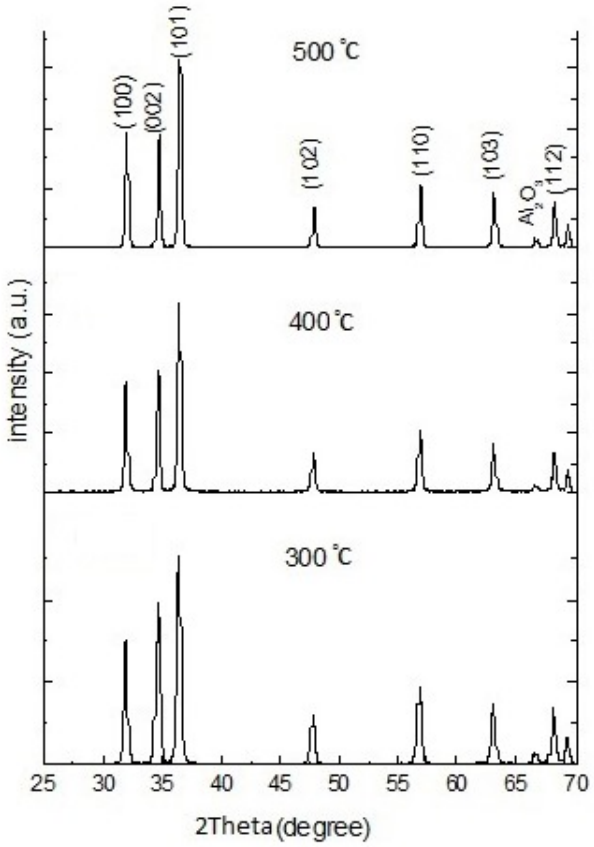

Fig. 3: XRD patterns of ZnO nanostructuresZnO nanostructures grown on α-Al_2O_3coated substrates atdifferent temperatures of 300; 400 and 500 °C.

3.3Photodegradation process

To understand the relationship between the structure and photocatalytic performance of ZnO samples, the photocatalytic activities of synthesized ZnO by different morphologies are evaluated in the degradation of Methylene Blue (MB). The photo-degradation of MBisdefined as the normalized change in its concentration (C/C_0) (Fig. 4). Fromthis figures, it can be seen that ZnOnanorods prepared at growth temperature of 300 °Cexhibit the highest photocatalyticefficiency.Photocatalytic reactionstake place at the interface between the catalyst and the organic pollutants [12]. Because the nanorodshave highersurface area than the cauliflower- like structures, and the electron transport is easier in an interconnected structure than in a lumped one [12], the photocatalytic property of ZnOnanorods is superior than other nanostructures.

The photocatalytic degradation of organic dyes byZnOcatalystunder UV irradiation

typically includes different mechanisms. First, the excitation of the ZnO, which includes excitation of the ZnO by light irradiation to form photogenerated electron/hole pairs. The second mechanism is based on the excitation of dye, in which the dye acts as a sensitizer of UV light and excited electrons will be transferred from the dye to an electron acceptor to become a cationic dye radical followed by self-degradation or degradation by the reactive oxidation species[13].

For comparison, the MB solution was also exposed to UV source in the absence of photocatalyst to examine its degradation by UV light.In this case, no degradation was observed even after long UV irradiation time. Therefore the degradation of MB is due to the presence of ZnO nanostructures as a catalyst and only UV irradiation has no degradation effect in the absence of ZnO nano structures. Another affecting parameter on photocatalytic efficiency is adsorption capacity. The ZnOnano rods present a porous and interconnected structure which permits the MB molecules to penetrate easily into the ZnO structure and therefore the amount of MB absorbed onto the photocatalyst, in comparison with cauliflower-like structures, increases.

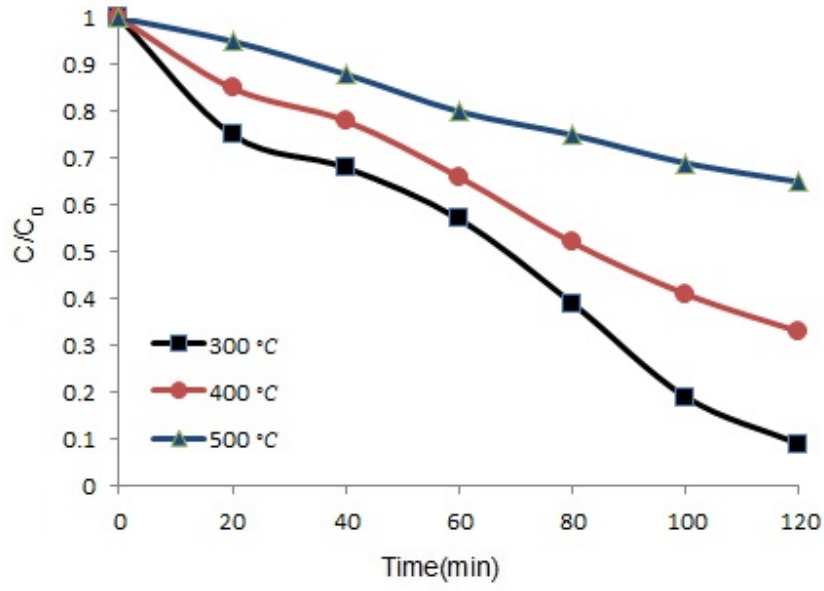

Fig. 4.Photo-degradation of MB aqueous solution degraded by ZnO nanostructures under UV light.ZnO nanostructures grown on α-Al_2O_3coated substrates at different temperatures of 300; 400 and 500 °C.

3.4 UV-VIS absorption spectra

The band gap energy (E_g) of ZnO nanostructures can be calculated from the UV-Vis spectra by Tauc plot of $(h\nu\alpha)^2$ versus ($h\nu$) and extrapolation of the linear portions of curves to energy axis according to equation 1[14]:

$(h\nu\alpha)^2 = A(h\nu - E_g)$..... (1)

Where $h\nu$ is photon energy, α is absorption coefficient, E_g is direct band gap energy, and A is proportional constant. Normally the obtained diffuse reflectance spectrum is converted to Kubelka-Munk function in which α in Tauc equation is substituted with $F(R_\infty)$ according to equation 2[15].

$(h\nu F(R\infty))^2 = A(h\nu - E_g)$.....(2)

The diffuse reflectance spectra were analyzed using Kubelka–Munk function. This function $F(R\infty)$ is related to the diffuse reflectance, $R\infty$, of the sample by the relation 3.

$$F(R\infty) = \frac{(1-R)^2}{2R} \quad \text{.....} \quad (3)$$

Here, $R\infty$ is the absolute value of reflectance and $F(R\infty)$ is equivalent to the absorption coefficient. Hence, according to Eq. 2 the indirect band gap of ZnO nanostructure was estimated by plotting $(h\nu F(R\infty))^2$ versus $h\nu$ in Fig. 5andwas found to decrease with an increase in growth temperature from 300 – 500 °C.The estimated optical band gaps of ZnO nanostructure synthesized at the growth temperatures of 300, 400 and 500 °C are about 3.29 eV, 3.25 eV and 3.22 eV, respectively. The position of the absorption spectra of ZnO sample synthesized at 300 °C is observed to shift towards the lower wavelength side compared with other two growth temperatures. The blue- shift indicates the decrease in size of the particle and increase in band gap energy [16]. The increase in the band gap or blue shift clearly explains the quantum confinement effect of ZnO nanostructures. In addition, the blue-shift of absorption edge can possibly be attributed to higher defect density on the surface of nanostructures with lower diameters [7]. Different defect concentrations are expected to provide new bound excitons with new binding energies which can result in spectral shift in nanostructures with different sizes [17].

3.5 Growth Mechanism

In order to understand the morphological changes with temperature, we need to discuss the growth mechanism of ZnOnanorods. Our growth model was likely governed by the mechanism similar to vapor –solid (VS) process. As schematically illustrated in Fig.1, the growth mechanism can be divided into two stages; (i) nucleation of ZnO clusters and (ii) growth of ZnO nanostructures. At room temperature, zinc acetate cannot be

completely dissociated in water and exists as $Zn(CH_3COO)_2(aq)$. During magnetic stirring when the temperature is increased, $Zn(CH3COO)_2$ can be hydrolyzed and forms $Zn(OH)(CH_3COO)$ as intermediate species according to reaction 4:

$Zn\ (CH_3COO)_2 + H_2O \rightarrow Zn\ (OH)\ (CH_3COO) + \ldots\ldots$ (4)

By increasing the temperature, the hydrated phaseis gradually evaporated together with water molecules. This phase is then condensed on crucible wall and the substrate, which is located on its top.So, Zn-O-Zn bond which plays the role of ZnO nuclei is formed according to reactions 5or 6. Schematic illustration of hydration and condensation of Zn ion complex is shown in Fig. 6.

$Zn\ (OH)\ (CH_3COO) + Zn\ (OH)\ (CH_3COO) \rightarrow Zn_2(O)\ (CH_3COO)_2 + H_2O$.....(5)

$Zn\ (CH_3COO)_2 + Zn\ (OH)\ (CH_3COO) \rightarrow Zn_2(O)\ (CH_3COO)_2 + CH_3COOH$..... (6)

$Zn_2(O)\ (CH_3COO)_2 \rightarrow ZnO + Zn\ (CH_3COO)_2$.....(7)

Once the nucleation is accomplished (reaction 7) on Al_2O_3 substrate, the particles can grow by addition of the intermediate species.

Fig. 2 indicates that as the growth temperature increases the mean length of the nanostructure decreases, while diameter increases. At processing temperature 300 °C, from the mean length and mean diameter, depicting rod -like morphology, while at higher growth temperatures the morphology shifts to cauliflower -like. For sample processed at 400 and 500°C, the morphology is such that several nanorods merge together from multiple nuclei due to an increased possibility of inter-particle collisions.

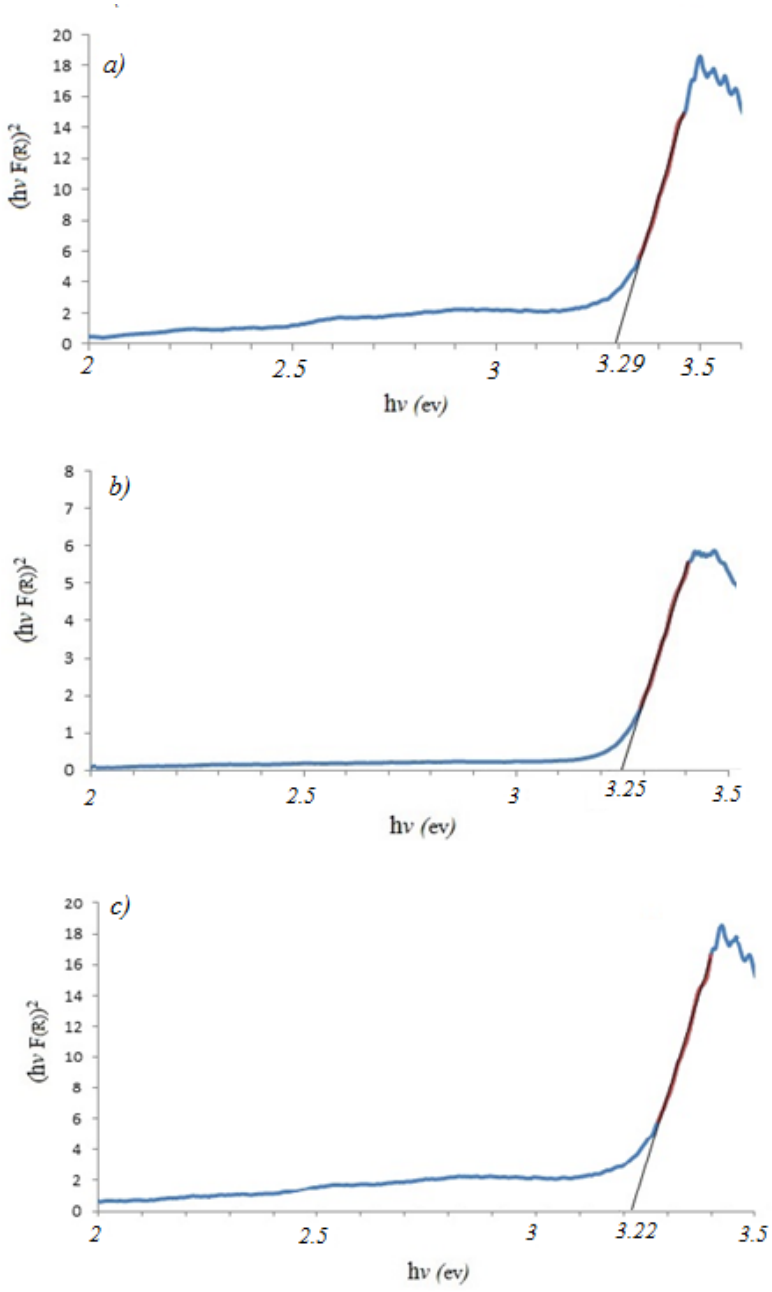

Fig. 5.Tauc plot of ZnO nanostructures at different growth temperatures: a) 300; b) 400 and c) 500 °C.

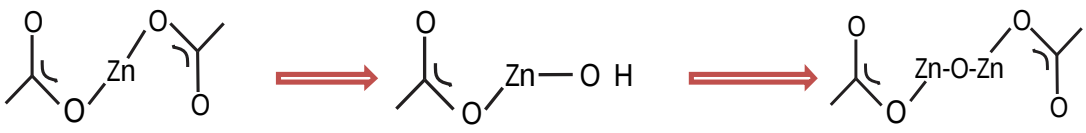

Fig. 6.Schematic illustration of hydration and condensation of Zn ion complex

Based on the formation of wire-like nanostructures might be controlled by kinetics during crystal growth, the probability of nucleation on the surface of a whisker is given by [18]:

$$P_N = Bexp\left(\frac{-\pi\sigma^2}{k^2T^2ln\alpha}\right) \quad \text{.....(7)}$$

Where P_N is the nucleation probability, σ is the surface energyof the whisker, T is absolute temperature, α the super saturation ratio determined by $\alpha=p/p_o$ where p is the actual vapour pressure and p_o is the equilibrium vapour pressure corresponding to temperature T; k is Boltzmann constant and B is a constant. In Eq. (7), temperature and supersaturation ratio are the parameters which are controlled by processing conditions. Higher the temperature and supersaturation ratio facilitate the2D nucleation, resulting in growth of plate like structures. Contrary, at low temperatures and small supersaturation ratio 1D nucleation is more possible [18]. This is in agreement with rod –like ZnO nanostructures in these experiments. As the growth temperature increases (Fig.2 b and c), ZnO morphology changes from nanorod to a cauliflower- like structure. The possible reason for these observed morphologies is the competition between nucleation rate and growth rate of ZnO crystals. At low temperatures, high nucleation rate and low growth rate in the radial direction lead to rod-like structure, whereas at higher temperature, lower nucleation rate and higher growth rate in the radial direction causethe ZnO can grow in both directions and 2D growth becomes dominant, resulting in cauliflower-like structure with a reduced aspect ratio as illustrated in Fig. 7.

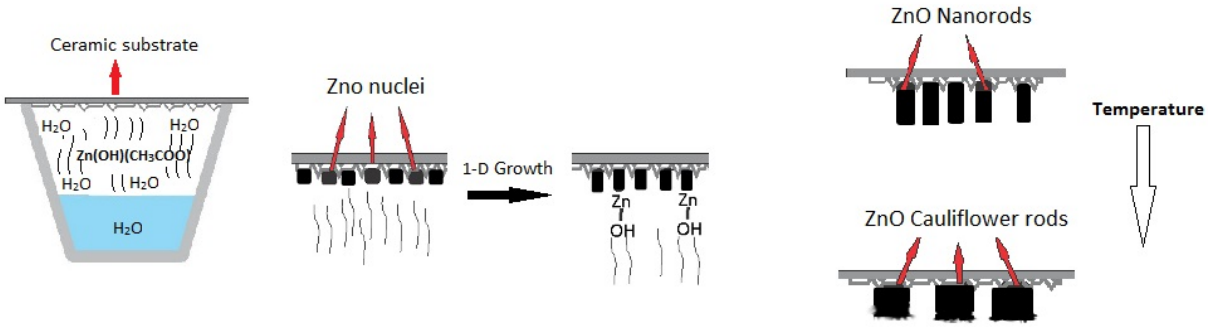

Fig. 7: The Scheme of the growth mechanism of ZnO particles as a function of the growth temperature.

3.6 Antifungal properties of ZnOnanorods

To study the antifungal properties, *Candida albicans* primary was cultured on Sabouraud dextrose agar medium. Yeast cells were counted and adjusted at 1×10^6 cell/mL by using Neubauer slide. The antifungal activity test of ZnOnanorods against *Candida albicans* under UV irradiation was evaluated

by broth micro dilution technique.It was observed that the prepared nanostructures diminish and inhibit the growth of cells (inhibitor zone around the disk) (Fig.8).Comparing the cell concentration on control substrate and ZnOnano structures grown on Al_2O_3substrate shows the highest antifungal activity of ZnOnanorod sprepared at 300 °C.

Considering the fact that ZnOnanorods can also eliminate the fungi cells without UV irradiation, the antifungal activity of ZnO is due to the generation of highly reactive oxygen species such as OH^-, O_2^{2-} and H_2O_2 as well as mechanical damage of the cell membrane[3, 19].

Fig. 9 displays the FE-SEM image of *Candida albicans* biofilms incubated on glass substrate as a control plate (Fig.9 a) and ZnOnanorods grown on Al_2O_3substrate after 30 min UV irradiation (Fig.9 b). Comparing the cell concentration on control glass substrate and ZnOnanorods grown on Al_2O_3substrate shows the antifungal activity of the ZnOnanorods.

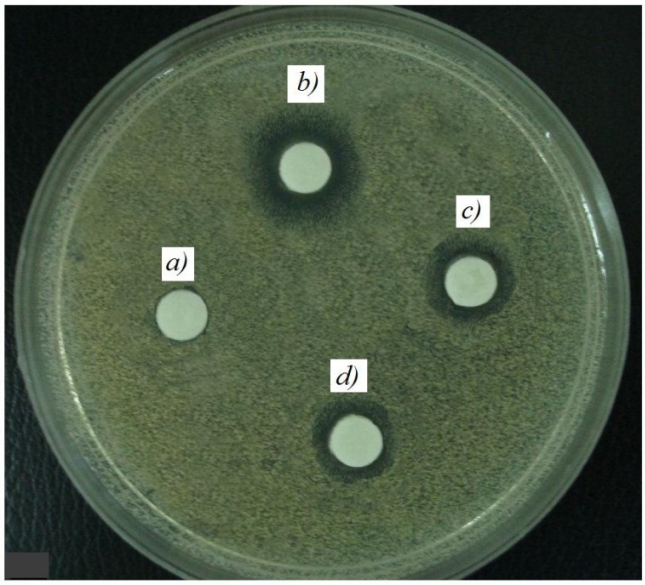

Fig. 8.Optical image of the grown cells around the plates including the antifungal nanostructures: a) blank control and plate treated by the grown nanostructure at b) 300; c) 400 and d) 500 °C.

As shown in Fig.9 b, the viability of the fungi has been suppressed considerably around the clusters of ZnOnanorods. It obviously demonstrates the antifungal activity of synthesized ZnOnanorods. The obtained results were confirmed by investigating the cell concentration around the antifungal agents by an optical imaging. As presented in optical image of grown cells (Fig. 8), an inhibitor zone around the disk (white area)

represents the inactivation effect of ZnO nanostructures in aqueous solution. It was detected that ZnOnanorods reduce and inhibit the growth of fungi, and their antifungal properties remained after 30 days such that no growth of fungi on the disk was observed. The results revealthat ZnOnanorods have high antifungalactivity in UV region.

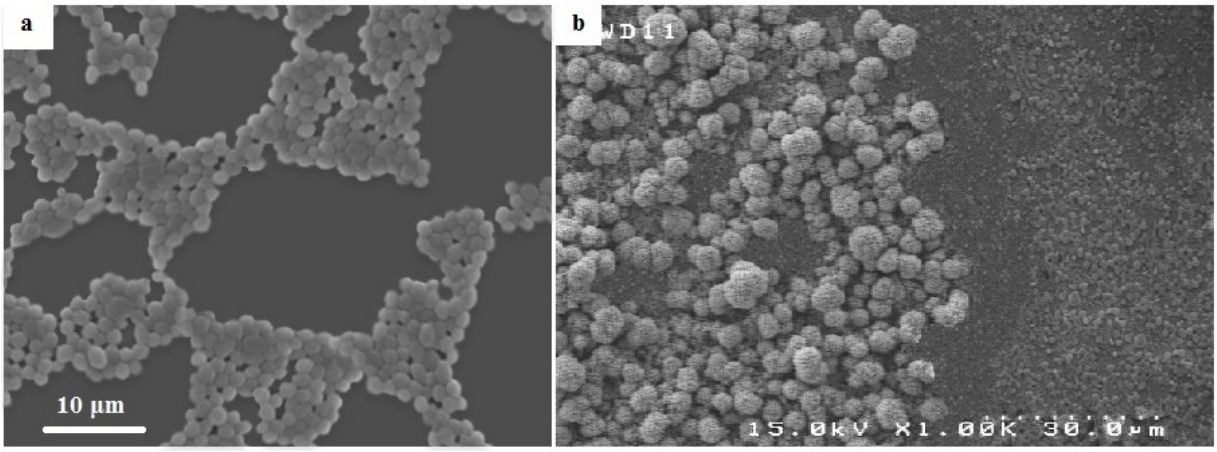

Fig. 9.FESEM image of incubated samples showing the (a) viability of the fungal cells on glass substrate (as a control plate) and (b) clusters of ZnOnanorods surrounded by fungal cells.

Considering the fact that ZnOnanorods can also eliminate the fungi cells without UV irradiation, the anti-fungal experiment was carried outin dark condition. As shown in Fig. 9, comparison of the relative number of viable cells on ZnOnanorods grown on Al_2O_3 substrate and the glass substrate (as the control sample) shows that the number of the cells is decreased on ZnOnanorods. This figure demonstrates that ZnOnanorods can decline the growth of fungi cells in the absence of UV light, but the irradiation of UV light plays a significant role on the antifungal rate.

The mechanism of antifungal activity of ZnO is considered to be due to several scenarios. One of the several alternative mechanisms suggest the generation of highly reactive oxygen species such as OH^-, O_2^{2-} and H_2O_2as described in the following[5, 20]:

When ZnOnanorodsare exposed to UV or visible light, electron-hole pairs ($e^- h^+$) can be created in conduction and valance band. The photogenerated holes split H_2O molecules (surrounding the ZnOnanorods) into OH^- and H^+.

$ZnO + photon(hv) \longrightarrow ZnO\text{-}e^-$ (conduction band) + $ZnO\text{-}h^+$(valence band) (8)

The photo generated holes create OH radicals according to reactions 2 and 3:

$ZnO\text{-}h^+ + H_2O \longrightarrow ZnO\text{-}OH^{\cdot} + H^+$ ..... (9)

$ZnO\text{-}h^+ + OH^- \longrightarrow ZnO\text{-}OH^{\cdot}$ ..... (10)

$OH^{\bullet}$ radicals created on the surface of microorganism are responsible for inactivating the biocells. The electrons

transform the dissolved oxygen molecules to superoxide radical anions ($^{\cdot}O_2^-$) which in turn produce hydrogen peroxide (H_2O_2) molecules according to following reactions:

$O_2 + e^- \longrightarrow {}^{\cdot}O_2^-$ .....(11)

${}^{\cdot}O_2^- + H^+ \longrightarrow HO_2^{\cdot}$ .....(12)

$HO_2^{\cdot} + H^+ + e^- \longrightarrow H_2O_2$ .....(13)

Since the hydroxyl radicals and superoxides are negatively charged particles, they cannot penetrate into the cell membrane and must remain in direct contact with the outer surface of the microorganism; however, the generated H_2O_2 can penetrate the cell membrane and kill the microorganism [8].

Another possible mechanism for antifungal effect of ZnO is mechanical damage of the cell membrane of microorganism by electrostatic interaction. This mechanical damage is based on surface roughness of ZnO. The abrasive surface of ZnO is due to surface defects[8].It was also suggested that the orientation of ZnO can affect the bioactivity, so randomly oriented ZnO nanowires show superior antibacterial activity compared with regularly oriented ZnO nanowires due to the different spatial arrangements of ZnO causing the biocidal activity[3, 8]. However, the exact mechanism of antifungal actions of different orientations of ZnOnanoarrays is not known.

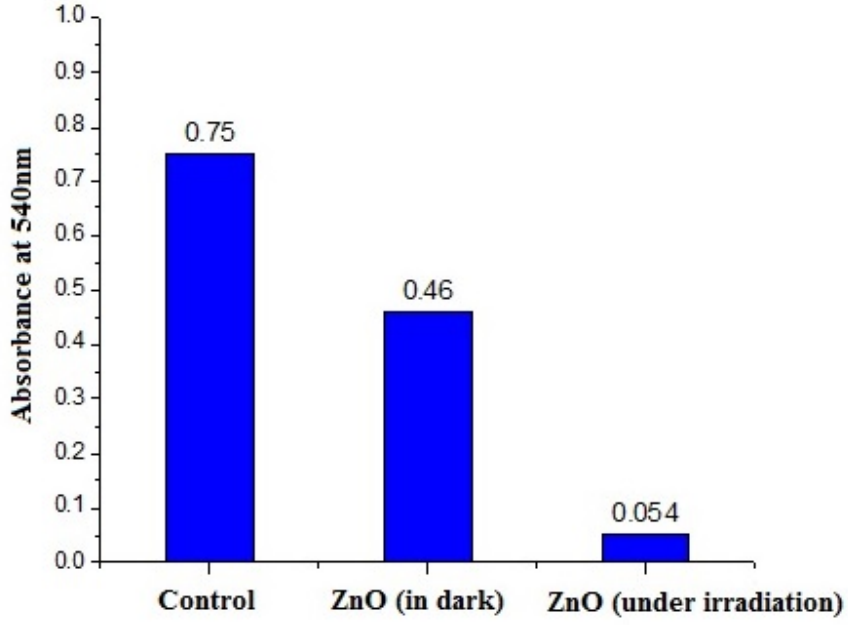

Fig. 10.Optical absorbance at the wavelength of 540 nm of yeast grown samples comparing of the relative number of viable cells on ZnOnanorods grown on Al_2O_3 substrate and the glass substrate (as the control sample).

CONCLUSIONS

Zinc Oxide nanostructures were synthesized on α-Al_2O_3 substrate via a simple novel method called "atmospheric pressure solution evaporation (APSE)" at 300, 400 and 500 °C. The growth temperature plays a significant role on morphology evolution of the grown products from nanorads to cauliflower- like structures. The X-ray diffraction patterns of ZnO nanostructures can be indexed as hexagonal Wurtzite structure without any impurity. According to XRD results, when the growth temperature is 300 °C, the intensity of (002) peak is higher than (100) peaks, which means that c-axis growth is dominant. However, when the growth temperature increases, the preferred growth direction changes to (100) direction, showing that the growth mode changes from 1D growth to 2D growth. The estimated optical band gaps of ZnO nanostructure synthesized at the growth temperatures of 300, 400 and 500 °C are about 3.29 eV, 3.25 eV and 3.22 eV, respectively. ZnOnanorods prepared at 300 °C exhibited the highest photocatalytic and antifungal activity.

REFERENCES

[1] Nair, M. G.; Nirmala, M.; Rekha, K.; Anukaliani, A., Structural, optical, photo catalytic and antibacterial activity of ZnO and Co doped ZnO nanoparticles. *Materials Letters* **2011,** 65, (12), 1797-1800.

[2] Zhang, H.; Feng, J.; Wang, J.; Zhang, M., Preparation of ZnO nanorods through wet chemical method. *Materials Letters* **2007,** 61, (30), 5202-5205.

[3] Manna, A. C., Synthesis, characterization, and antimicrobial activity of zinc oxide nanoparticles. In *Nano-Antimicrobials*, Springer: 2012; pp 151-180.

[4] Liu, C.; Li, H.; Jie, W.; Zhang, X.; Yu, D., Preparation of ZnO cluster and rod-like whiskers through hydrothermal methods. *Materials Letters* **2006,** 60, (11), 1394-1398.

[5] Liu, J.; Huang, X.; Duan, J.; Ai, H.; Tu, P., A low-temperature synthesis of multiwhisker-based zinc oxide micron crystals. *Materials Letters* **2005,** 59, (28), 3710-3714.

[6] Breedon, M.; Rahmani, M. B.; Keshmiri, S.-H.; Wlodarski, W.; Kalantar-zadeh, K., Aqueous synthesis of interconnected ZnO nanowires using spray pyrolysis deposited seed layers. *Materials Letters* **2010,** 64, (3), 291-294.

[7] Eskandari, M.; Ahmadi, V.; Ahmadi, S., Low temperature synthesis of ZnO

nanorods by using PVP and their characterization. *Physica B: Condensed Matter* **2009,** 404, (14), 1924-1928.

[8] Momen, M. H.; Amadeh, A.; Sohi, M. H.; Moghanlou, Y., Photocatalytic properties of ZnO nanostructures grown via a novel atmospheric pressure solution evaporation method. *Materials Science and Engineering: B* **2014,** 190, 66-74.

[9] Li, G.; Hu, T.; Pan, G.; Yan, T.; Gao, X.; Zhu, H., Morphology− function relationship of ZnO: polar planes, oxygen vacancies, and activity. *The Journal of Physical Chemistry C* **2008,** 112, (31), 11859-11864.

[10] Fang, Y.; Wang, Y.; Wan, Y.; Wang, Z.; Sha, J., Detailed study on photoluminescence property and growth mechanism of ZnO nanowire arrays grown by thermal evaporation. *The Journal of Physical Chemistry C* **2010,** 114, (29), 12469-12476.

[11] Habibpanah, A. A.; Pourhashem, S.; Sarpoolaky, H., Preparation and characterization of photocatalytic titania–alumina composite membranes by sol–gel methods. *Journal of the European Ceramic Society* **2011,** 31, (15), 2867-2875.

[12] Kim, S.-J.; Park, D.-W., Preparation of ZnO nanopowders by thermal plasma and characterization of photo-catalytic property. *Applied Surface Science* **2009,** 255, (10), 5363-5367.

[13] Shidpour, R.; Simchi, A.; Ghanbari, F.; Vossoughi, M., Photo-degradation of organic dye by zinc oxide nanosystems with special defect structure: Effect of the morphology and annealing temperature. *Applied Catalysis A: General* **2014,** 472, 198-204.

[14] Anderson, C.; Bard, A. J., Improved photocatalytic activity and characterization of mixed TiO2/SiO2 and TiO2/Al2O3 materials. *The Journal of Physical Chemistry B* **1997,** 101, (14), 2611-2616.

[15] Simmons, B. A.; Li, S.; John, V. T.; McPherson, G. L.; Bose, A.; Zhou, W.; He, J., Morphology of CdS nanocrystals synthesized in a mixed surfactant system. *Nano Letters* **2002,** 2, (4), 263-268.

[16] Saravanan, R.; Thirumal, E.; Gupta, V.; Narayanan, V.; Stephen, A., The photocatalytic activity of ZnO prepared by simple thermal decomposition method at various

temperatures. *Journal of Molecular Liquids* **2013,** 177, 394-401.

[17] Djurišić, A. B.; Leung, Y. H., Optical properties of ZnO nanostructures. *Small* **2006,** 2, (8-9), 944-961.

[18] Shakti, N.; Prakash, A.; Mandal, T.; Katiyar, M., Processing temperature dependent morphological and optical properties of ZnO nanorods. *Materials Science in Semiconductor Processing* **2014,** 20, 55-60.

[19] Padmavathy, N.; Vijayaraghavan, R., Enhanced bioactivity of ZnO nanoparticles—an antimicrobial study. *Science and Technology of Advanced Materials* **2008,** 9, (3), 035004.

[20] Jalal, R.; Goharshadi, E. K.; Abareshi, M.; Moosavi, M.; Yousefi, A.; Nancarrow, P., ZnO nanofluids: green synthesis, characterization, and antibacterial activity. *Materials Chemistry and Physics* **2010,** 121, (1), 198-201.